HydroSed2D: A Two-Dimensional Numerical Model for Hydrodynamics and Sediment Transport

Version 1.0

by

Xiaofeng Liu

liu19@illinois.edu

http://vtchl.uiuc.edu/ liu19

Postdoctoral Research Associate

Ven Te Chow Hydrosystems Laboratory
Department of Civil and Environmental Engineering
University of Illinois at Urbana and Champaign, IL

2009.1

Contents

License

Chapter 1

Introduction

The code HydroSed2D stands for two-dimensional hydrodynamics and sediment transport. This code originates from my master thesis back in Peking University in P.R. China (Liu, 2003). I got a lot of help from Professor Alistair Borthwick of Oxford University, UK. He has a similar code which solves the shallow water equation based on quadtree mesh structure. HydroSed2D is part of my Ph.D. work at University of Illinois at Urbana-Champaign (UIUC). The extension and modification include: (1) Unstructured mesh for complicated domain and real world applications (2) Sediment transport which implements both quasi-steady and coupled approaches (Liu and Garcia, 2008c) (3) Balanced scheme for slope term (Liu and Garcia, 2008a). In the current release of the code, only the quasi-steady approach for sediment transport is implemented.

HydroSed2D has been used for several projects, such as dam break flow (Liu, 2003), river erosion (Liu and Parker, 2009), and local scour (Liu and Garcia, 2008c).

Before using the code, the reader should be aware of the limitations of HydroSed2D:

- Shallow water assumption. Vertical movement of water is ignored
- Small time step due to the explicit nature of the numerical scheme
- Wet-dry interface handling needs improvement
- Some part of the code needs to be reorganized
- Although I will try my best, the code is not so well documented since I am maintaining it using my spare time. Request of new features and timely response are not guaranteed from the author

If you do use this code for your research or engineering application, please let me know. I would also appreciate your comments and help to make improvement. People who are interested to collaborate with me can send email to liu19@illinois.edu.

HydroSed2D is an open source code released under GNU General Public License (GPL).

Chapter 2

Numerical Model

In this chapter, the details of the numerical model are described. Most of the governing equations can be found in Liu and Garcia (2008c) and Liu (2008).

2.1 Hydrodynamic Equations

The hydrodynamic part of the code is to solve the shallow water equations on unstructured mesh. The non-linear shallow water equations have the form

$$\frac{\partial \xi}{\partial t} + \frac{\partial (uh)}{\partial x} + \frac{\partial (vh)}{\partial y} = 0, \tag{2.1}$$

$$\frac{\partial (uh)}{\partial t} + \frac{\partial (u^2 h)}{\partial x} + \frac{\partial (uvh)}{\partial y} - \nu \left(\frac{\partial (hu_x)}{\partial x} + \frac{\partial (hu_y)}{\partial y} \right) = \frac{\tau_{wx} - \tau_{bx}}{\rho} - gh\frac{\partial \xi}{\partial x} + hfv, \tag{2.2}$$

$$\frac{\partial (vh)}{\partial t} + \frac{\partial (uvh)}{\partial x} + \frac{\partial (v^2 h)}{\partial y} - \nu \left(\frac{\partial (hv_x)}{\partial x} + \frac{\partial (hv_y)}{\partial y} \right) = \frac{\tau_{wy} - \tau_{by}}{\rho} - gh\frac{\partial \xi}{\partial y} - hfu, \tag{2.3}$$

where ξ is the free surface elevation above the still water level h_s, h is the total water depth $(= h_s + \xi)$, u and v are the depth-averaged velocities in the x and y directions, respectively, t is time, τ_{wx} and τ_{wy} are wind shear stresses, τ_{bx} and τ_{by} are bottom friction forces, ν is the viscosity, g is the gravity constant, and f is the Coriolis parameter.

In order to obtain the hyperbolic formulation, the $gh\frac{\partial \xi}{\partial x}$ and $gh\frac{\partial \xi}{\partial y}$ terms are split according to

$$gh\frac{\partial \xi}{\partial x} = \frac{1}{2}g\frac{\partial (\xi^2 + 2\xi h_s)}{\partial x} + g\xi S_{ox}, \tag{2.4}$$

$$gh\frac{\partial \xi}{\partial y} = \frac{1}{2}g\frac{\partial (\xi^2 + 2\xi h_s)}{\partial y} + g\xi S_{oy}, \tag{2.5}$$

where S_{ox} and S_{oy} are bed slopes in x and y directions, respectively.

Using this splitting, the shallow water equations (Eqns. 2.1, 2.2, and 2.3) can be rewritten (Rogers et al., 2001, 2003) as

$$\frac{\partial \xi}{\partial t}+\frac{\partial (uh)}{\partial x}+\frac{\partial (vh)}{\partial y}=0, \tag{2.6}$$

$$\begin{aligned}\frac{\partial (uh)}{\partial t}+\frac{\partial (u^2h+\frac{1}{2}g(\xi^2+2\xi h_s))}{\partial x}+\frac{\partial (uvh)}{\partial y}-\nu\left(\frac{\partial (hu_x)}{\partial x}+\frac{\partial (hu_y)}{\partial y}\right)\\ =\frac{\tau_{wx}-\tau_{bx}}{\rho}-g\xi S_{ox}+hfv,\end{aligned} \tag{2.7}$$

$$\begin{aligned}\frac{\partial (vh)}{\partial t}+\frac{\partial (uvh)}{\partial x}+\frac{\partial (v^2h+\frac{1}{2}g(\xi^2+2\xi h_s))}{\partial y}-\nu\left(\frac{\partial (hv_x)}{\partial x}+\frac{\partial (hv_y)}{\partial y}\right)\\ =\frac{\tau_{wy}-\tau_{by}}{\rho}-g\xi S_{oy}-hfv.\end{aligned} \tag{2.8}$$

2.2 Sediment Transport Equations

The sediment transport rate formulas implemented are Grass formula (Grass, 1981) and MPM formula (Meyer-Peter and Muller, 1948). The implementation of other formulas is straight forward since the shear stress is given by the hydrodynamic part of the code and can be used as the driving force for sediment movement.

The Grass formula (Grass, 1981), which relates the bed load to velocities, has the form

$$q_{sx}=Au\left(u^2+v^2\right)^{\frac{m-1}{2}}, \tag{2.9}$$

$$q_{sy}=Av\left(u^2+v^2\right)^{\frac{m-1}{2}}, \tag{2.10}$$

where A and m are parameters determined by the properties of the sediment. In this paper, $A=0.001$ and $m=3$ are chosen which correspond to fine sand. q_{sx} and q_{sy} are the sediment transport rates in the x and y directions, respectively.

The conservation law of the sediment is described by the Exner equation,

$$\frac{\partial z}{\partial t}+\frac{1}{1-\epsilon_0}\left(\frac{\partial q_{sx}}{\partial x}+\frac{\partial q_{sy}}{\partial y}\right)=0, \tag{2.11}$$

where z is the bed elevation, and ϵ_0 is the sediment porosity.

2.3 Numerical method of the model

Integrating the governing equations over the domain Ω and using Green's theorem, the integral form of the governing equations can be written as

$$\frac{\partial}{\partial t}\iint_{\Omega}\mathbf{Q}\,\mathrm{d}\Omega+\oint_S \mathbf{F}\cdot\mathbf{n}\mathrm{d}S=\iint_{\Omega}\mathbf{H}\mathrm{d}\Omega, \tag{2.12}$$

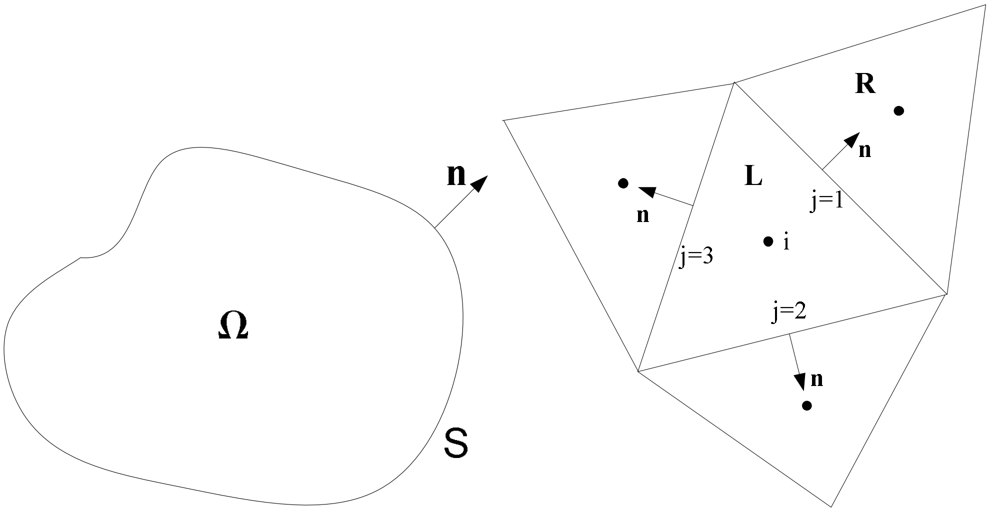

(a) (b)

Figure 2.1: Scheme of the computational domain: (a) control volume (b) triangle mesh

where Ω is the domain of interest, S is the boundary of Ω (see Fig. 2.1(a)), $\mathbf{n}$ is the outward surface normal vector of S, $\mathbf{Q}$ is the conservative variables vector, $\mathbf{F}$ is the flux vector, and $\mathbf{H}$ is the source term vector. The forms of $\mathbf{Q}$, $\mathbf{F}$, and $\mathbf{H}$ will be listed in the following sections. $\mathbf{F}$ can be split into viscous and inviscid flux components as

$$\mathbf{F}\cdot\mathbf{n} = F^I - F^V = \left(f^I - \nu f^V\right) n_x + \left(g^I - \nu g^V\right) n_y, \tag{2.13}$$

where n_x and n_y are the Cartesian components of the normal vector ($\sqrt{n_x^2+n_y^2} = |\mathbf{n}|$=1), and superscripts I and V denote invicid and viscous components, respectively.

In quasi-steady approach, the SWEs are analyzed separately from the Exner equation. For the SWEs, $\mathbf{Q}$, $\mathbf{F}$ and $\mathbf{H}$ have the forms

$$\mathbf{Q} = \begin{bmatrix} \xi \\ uh \\ vh \end{bmatrix} \quad f^I = \begin{bmatrix} uh \\ u^2h + g(\xi^2 + 2\xi h_s)/2 \\ uvh \end{bmatrix} \quad g^I = \begin{bmatrix} vh \\ uvh \\ v^2h + g(\xi^2 + 2\xi h_s)/2 \end{bmatrix}$$

$$f^V = \begin{bmatrix} 0 \\ h\frac{\partial u}{\partial x} \\ h\frac{\partial v}{\partial x} \end{bmatrix} \qquad g^V = \begin{bmatrix} 0 \\ h\frac{\partial u}{\partial y} \\ h\frac{\partial v}{\partial y} \end{bmatrix} \qquad \mathbf{H} = \begin{bmatrix} 0 \\ \frac{\tau_{wx}-\tau_{bx}}{\rho} - g\xi S_{ox} + hfv \\ \frac{\tau_{wy}-\tau_{by}}{\rho} - g\xi S_{oy} - hfu \end{bmatrix}. \tag{2.14}$$

The Exner equation is also descretized using the FVM and Green theorem as in Eq. 2.12. However, the Godunov scheme is not used here simply because the sediment transport rate is not an explicit function of the bed elevation z and therefore the Jacobian matrix (only one element in this case) can not be evaluated. The fluxes across the cell interfaces are calculated using the variable values at the edges. The variable values at the edges are obtained via inverse distance weighted average method. For the Exner equation, $\mathbf{Q}$, $\mathbf{F}$, and $\mathbf{H}$ have the forms

$$\mathbf{Q} = z \quad \mathbf{F} \cdot \mathbf{n} = \frac{1}{1-\epsilon_0}\left(q_{sx}n_x + q_{sy}n_y\right) \quad \mathbf{H} = 0. \tag{2.15}$$

2.4 Evaluation of numerical fluxes

The fluxes $\mathbf{F}$ across the interface between each two triangles are separated into inviscid and viscous fluxes. For the inviscid fluxes, one-dimensional Riemann problem is extended to two dimensions. Analytical or approximate solvers of Riemann problem can be used to evaluate the fluxes. For the viscous fluxes, the velocity gradient is evaluated at the edge's center and then used to calculate the viscous fluxes.

The analytical solver of the Riemann problem is slow when compared to the approximate ones. Among the many choices of approximate solvers, Roe's approach (Roe, 1981, 1986) is used in this paper. The inter-cell inviscid flux $\mathbf{F}^I_{i,j}$ by Roe's solver can be written as

$$\mathbf{F}^I_{i,j} = \frac{1}{2}\left[\mathbf{F}^I(Q^+_{i,j}) + \mathbf{F}^I(Q^-_{i,j}) - |A|\left(\mathbf{Q}^+_{i,j} - \mathbf{Q}^-_{i,j}\right)\right], \tag{2.16}$$

$$|A| = R\,|\Lambda|\,L, \tag{2.17}$$

where $\mathbf{Q}^+_{i,j}$ and $\mathbf{Q}^+_{i,j}$ are reconstructed Riemann state variables on the right and left sides, respectively. The flux Jacobian matrix, A, is defined by

$$A = \frac{\partial \mathbf{F} \cdot \mathbf{n}}{\partial \mathbf{Q}}. \tag{2.18}$$

R and L are the right and left eigenvector matrices, and $|\Lambda|$ is a diagonal matrix of the absolute values of the eigenvalues of A.

For the quasi-steady approach, the flux Jacobian of the two-dimensional SWEs system without the Exner equation is listed below.

$$A = \frac{\partial \mathbf{F} \cdot \mathbf{n}}{\partial \mathbf{Q}} = \begin{bmatrix} 0 & n_x & n_y \\ (c^2-u^2)n_x - uvn_y & 2un_x + vn_y & un_y \\ -uvn_x + (c^2-v^2)n_y & vn_x & un_x + 2vn_y \end{bmatrix}. \tag{2.19}$$

The three distinct eigenvalues of A (by hyperbolicity of the system) are

$$\lambda^{(1)} = un_x + vn_y, \quad \lambda^{(2)} = un_x + vn_y - c, \quad \lambda^{(3)} = un_x + vn_y + c, \tag{2.20}$$

and the left and right eigenvector matrices are

$$R = \begin{bmatrix} 0 & 1 & 1 \\ n_y & u - cn_x & u + cn_x \\ -n_x & v - cn_y & v + cn_y \end{bmatrix}, \quad L = \begin{bmatrix} -(un_y - vn_x) & n_y & -n_x \\ \frac{un_x+vn_y}{2c} + \frac{1}{2} & \frac{-n_x}{2c} & \frac{-n_y}{2c} \\ -\frac{un_x+vn_y}{2c} + \frac{1}{2} & \frac{n_x}{2c} & \frac{n_y}{2c} \end{bmatrix}. \tag{2.21}$$

The Riemann state variables u, v, and c on the face boundaries which are needed to calculate the flux are given by Roe's average as

$$u = \frac{u^+\sqrt{h^+} + u^-\sqrt{h^-}}{\sqrt{h^+} + \sqrt{h^-}}, \quad v = \frac{v^+\sqrt{h^+} + v^-\sqrt{h^-}}{\sqrt{h^+} + \sqrt{h^-}}, \quad c = \sqrt{\frac{g(h^+ + h^-)}{2}}. \tag{2.22}$$

The superscripts $+$ and $-$ refer to the right and left side of the edge. The limitation of Roe's average is that it is not easy to deal with dry-wet interfaces. This happens when the model is applied to tidal flow at a beach or dam breaks over dry land.

The viscous fluxes are calculated directly using the velocity gradient at the boundary. The effect of viscous fluxes might not be significant for the applications presented in this paper. However, since no-slip conditions are used for wall boundaries, viscous fluxes are included in the model to be consistent. Furthermore, turbulence, which has a great effect on the transport of sediment, will be modeled in the future through the addition of a turbulent eddy viscosity term.

2.5 Time integration

The time integration used in the paper is similar to the method proposed by Anastasiou and Chan (1997),

$$\left.\frac{\partial(VQ)}{\partial t}\right|_i^{n+1} = -\oint_{S_i} \mathbf{F}_i^n \cdot \mathbf{n} dS + V_i^n H_i^n, \tag{2.23}$$

$$Q_i^{n+1} = Q_i^n + \frac{\Delta t}{V_i^n}\left(\alpha \left.\frac{\partial(VQ)}{\partial t}\right|_i^{n+1} + (1-\alpha)\left.\frac{\partial(VQ)}{\partial t}\right|_i^{n}\right). \tag{2.24}$$

when $\alpha = 0$, it becomes the Euler explicit scheme, while $\alpha = 1$ results in a first order Euler implicit method. For the explicit scheme, which is used in this paper, the time step is restricted by the Courant-Friedrichs-Lewy (CFL) condition. As in Yoon and Kang (2004), the following formula is used to determine the maximum time step allowed,

$$\Delta t \leq \min_i \left(\frac{R_i}{2\max_j(\sqrt{u^2+v^2}+c)_{ij}}\right), \tag{2.25}$$

where R_i is the nearest distance from the centroid of triangle i to its vertices. The minimum is taken for all the triangles in the computational domain while the maximum is taken for the three neighboring triangles of triangle i (see Fig. 2.1(b)).

2.6 Boundary conditions

For the hydrodynamic part of the model, the boundary conditions are the same as in Anastasiou and Chan (1997) and Rogers et al. (2001). Those boundary conditions are briefly listed below. For the sediment transport, the conditions on the boundary are also discussed.

2.6.1 Walls

For the wall boundary, the no-slip condition is applied. For sediment transport, the flux through the wall is also set to be zero which means no sediment particle will go through the solid boundary.

2.6.2 Open boundaries

Conditions for the open boundaries, including inlet and outlet, are specified using the Riemann invariants

$$(u, v)_I \cdot \mathbf{n} + 2\sqrt{gh_I} = (u, v)_B \cdot \mathbf{n} + 2\sqrt{gh_B}, \tag{2.26}$$

where subscripts I and B refer to the interface and the boundary.

For subcritical flow, if water depth h_B is specified, then

$$(u, v)_B \cdot \mathbf{n} = (u, v)_I \cdot \mathbf{n} + 2\sqrt{gh_I} - 2\sqrt{gh_B}, \tag{2.27}$$

and if velocity is specified, then

$$h_B = \frac{\left[(u, v)_I \cdot \mathbf{n} + 2\sqrt{gh_I} - (u, v)_B \cdot \mathbf{n}\right]^2}{4g}. \tag{2.28}$$

Sometimes, the water discharge $q_w = h_B\left[(u, v)_B \cdot \mathbf{n}\right]$ is specified. For this case, Eq. 2.26 can be rewritten as

$$(u, v)_I \cdot \mathbf{n} + 2\sqrt{gh_I} = \frac{q_w}{h_B} + 2\sqrt{gh_B}. \tag{2.29}$$

A numerical method can be used to solve h_B and then $(u, v)_B \cdot \mathbf{n} = q_w/h_B$.

For the supercritical inlet, both the velocity vector and water depth should be specified. For the supercritical outlet, no boundary condition is needed and the velocity vector and water depth on the boundary is the same as those in the adjacent interior.

For the sediment transport rate, the sediment flux on the inlet is specified as the sediment feed rate. On the outlet, the sediment flux is set as zero gradient.

Chapter 3

Examples

In this chapter, some examples are shown.

3.1 1D Transcritical Flow

This is a test case proposed in Goutal and Maurel (1997). It is for the one-dimensional steady flow in a 25m long, unit width channel with a bump defined by

$$Z_b(x) = \begin{cases} 0.2 - 0.05(x-10)^2 & \text{if } 8 < x < 12 \\ 0 & \text{otherwise} \end{cases} \quad (3.1)$$

where x is the distance along the channel. In order to run this case, the channel bottom has to be hardwired in the code (in the subroutine *interp_Elevation*).

Depending on the boundary conditions, the flow could be subcritical, transcritical (with and without shock). These three cases are presented here.

- Subcritical flow: A discharge per unit width of q = 4.42 m^2/s was imposed at the upstream boundary and h = 2 m was specified as the downstream boundary condition.
- Transcritical flow without a shock: A discharge per unit width of q = 1.53 m^2/s was imposed at the upstream boundary and free stream was specified as the downstream boundary condition.
- Transcritical flow with a shock: A discharge per unit width of q = 0.18 m^2/s was imposed at the upstream boundary and h = 0.33 m was specified as the downstream boundary condition.

3.2 2D Dam Break Flow over a Hump

For a domain [0,2] by [0,1], the bottom surface is given by

$$Z_b(x,y) = 0.5\exp[-50((x-0.5)^2 + (y-0.5)^2)] \quad (3.2)$$

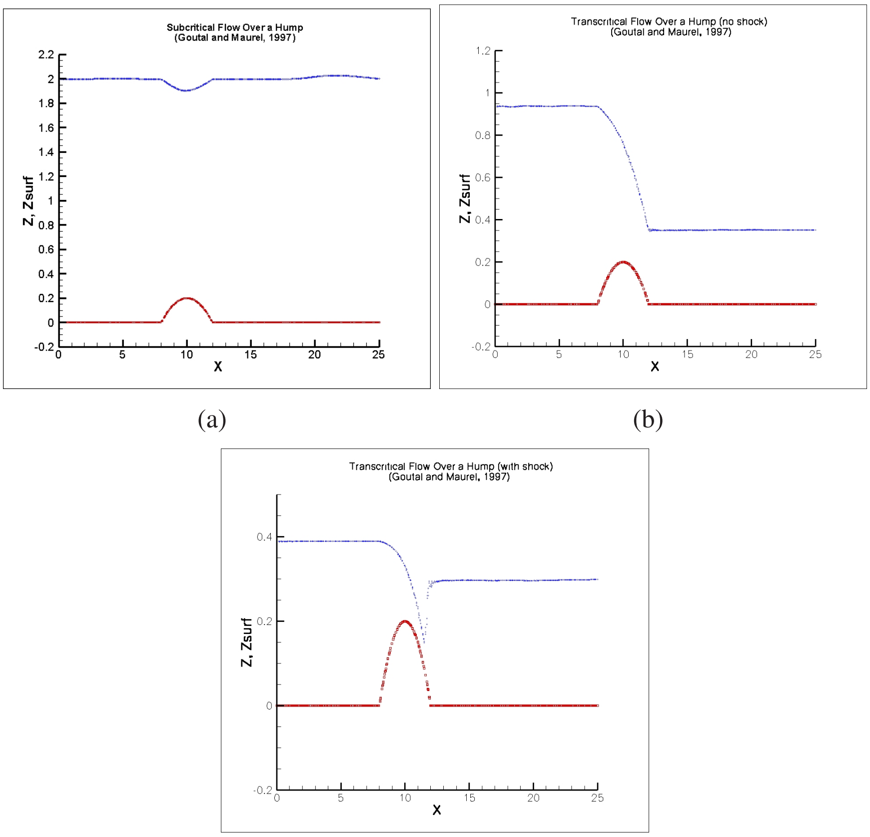

(a) (b) (c)

Figure 3.1: 1D Transcritical Flow Simulations: (a) Subcritical Flow over a Hump (b) Transcritical Flow over a Hump (No Shock) (c) Transcritical Flow over a Hump (with Shock)

The initial water surface elevation in the domain is 1 m, except in the area where $0.05 < x < 0.15$ which has a water surface elevation of 1.05 m. Figure 3.2 shows the water surface at time t = 0.2 s.

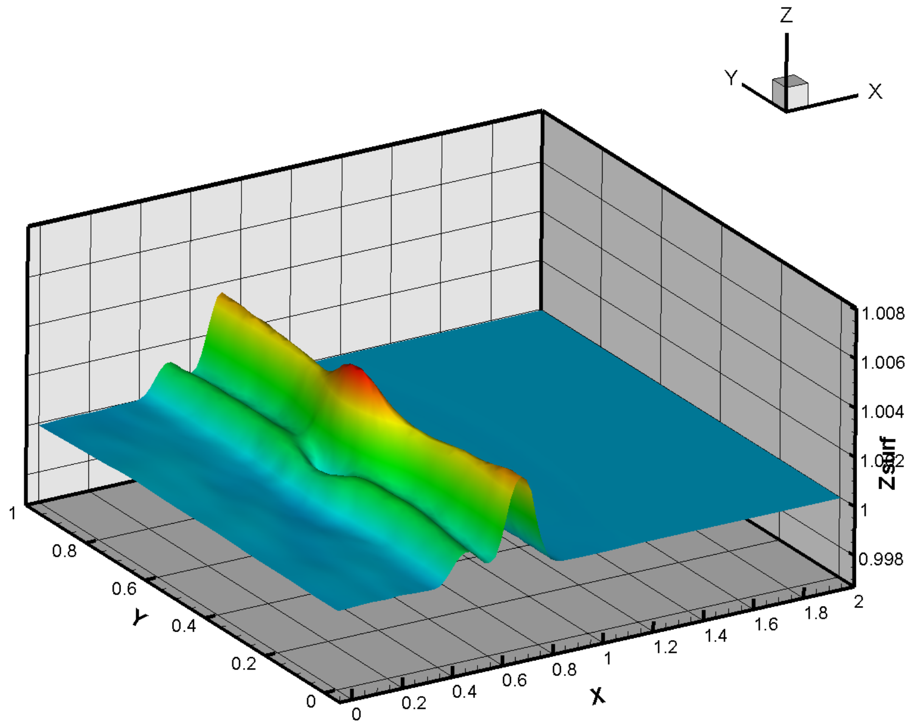

Figure 3.2: Flow over a hump (t = 0.2 s)

3.3 Flow around Spur Dykes

This example shows the flow structures around three spur dykes. Overall, the flow patterns are correct. However, due to the hydrostatic and shallow water assumptions, the three-dimensional structures and the related features are impossible to be resolved using HydroSed2D. Full three-dimensional computational fluid dynamic (CFD) models with the capability to capture free water surface can be used to fulfill this task (Liu and Garcia, 2008b).

Figure 3.3 shows the water surface and velocity.

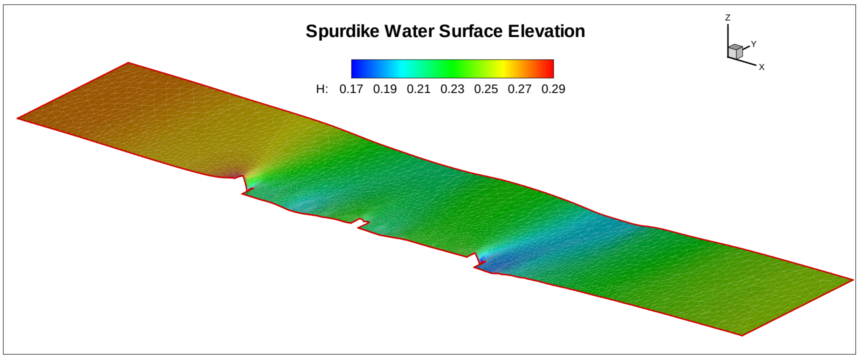

(a)

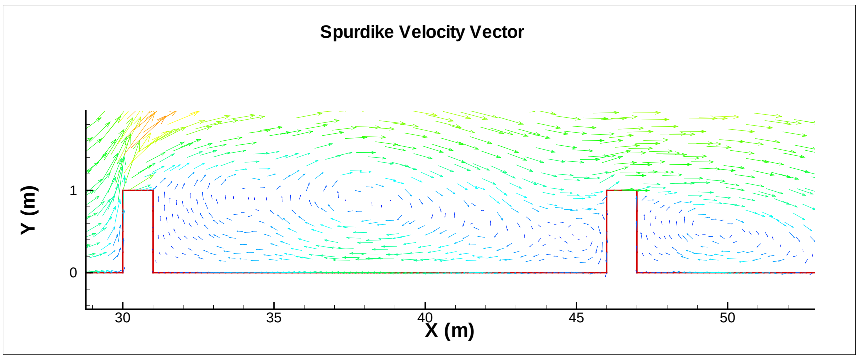

(b)

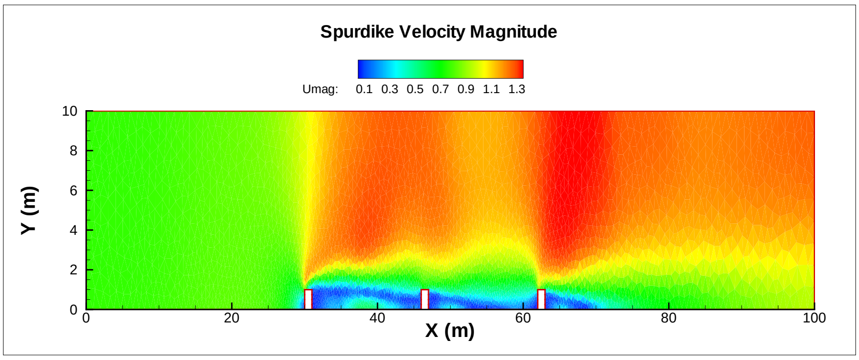

(c)

Figure 3.3: Channel Flow around Spurdikes: (a) Water Surface (b) Velocity Vectors (c) Velocity Magnitude

3.4 Movement of a Sediment Hump

This example taken from Hudson and Sweby (2005) which shows the ability of HydroSed2D to predict the sediment movement under the force of flow shear. The channel is 1500 m by 1000 m. The bottom elevation of the channel is given by

$$Z_b(x) = \begin{cases} \sin^2\left(\frac{\pi(x-500)}{200}\right)\sin^2\left(\frac{\pi(y-400)}{200}\right) & \text{if } 500 < x < 700, \quad 400 < y < 600 \\ 0 & \text{otherwise} \end{cases} \tag{3.3}$$

The unit width flow discharge is 10 m^2/s.

Figure 3.4 shows the sediment hump after one hour.

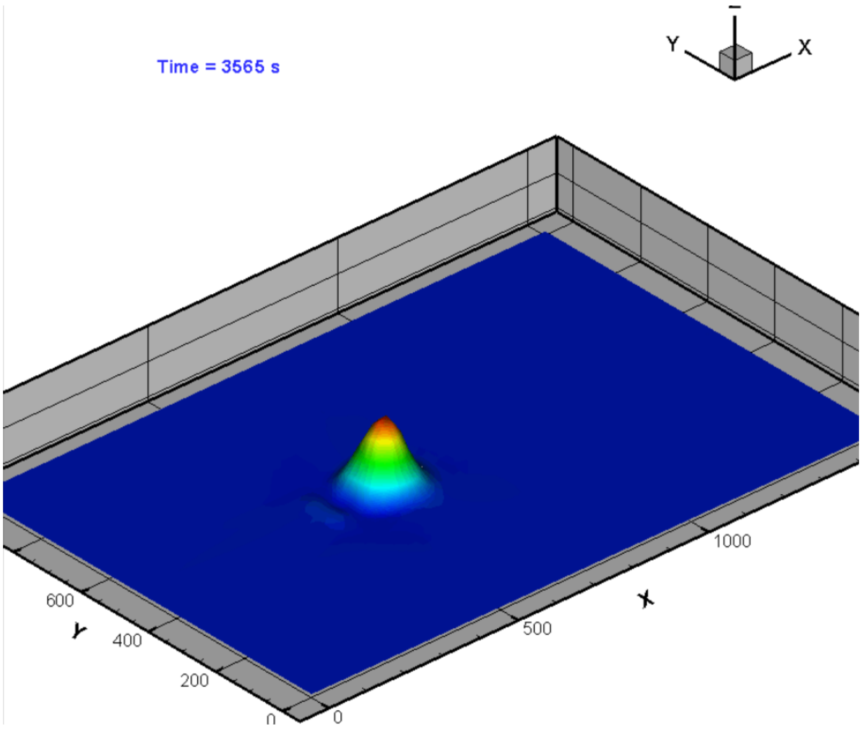

Figure 3.4: Movement of a Sediment Hump (t = 1 hour)

Chapter 4

Mesh Generation and Additional Tools

4.1 Mesh Generation

Two types of mesh are supported in HydroSed2D v1.0, namely Fluent Gambit neutral format and GMSH format (Geuzaine and Remacle, 2009). Before we proceed to introduce how to generate meshes using both software, we need to specify the boundary condition code. In HydroSed2D, there are basically three boundary conditions: inlet, outlet, and wall. They are distinguished by their codes,i.e., 1 for inlet, 2 for outlet, and 3 for wall. Code 4 is reserved for internal edges and therefore it is not valid to specify any boundary as code 4.

4.1.1 Gambit

Gambit is Fluent's geometry and mesh generation software. The reader is advised to consult its manual for details. Since there is no interface for export Gambit mesh to HydroSed2D, we use its neutral format. However, the boundaries needs to be changed accordingly. For example, in the author's version of Gambit, all boundaries are flagged as ”6”. They have to be modified to 1, 2, or 3 according to their types.

4.1.2 GMSH

Gmsh is an automatic 3D finite element grid generator with a built-in CAD engine and post-processor. However, it can also generate 2D meshes. It is a simple tool for problems with parametric input and advanced visualization capabilities. I have used GMSH for simple geometries to generate triangular unstructured meshes. The boundary types are specified in the ”geo” definition file.

4.2 Additional Tools

In this section, some additional tools are introduced. They are used to help set up the simulation cases, such as elevation data interpolation.

4.2.1 DEM Data Interpolations

Since the mesh generated from Gambit and GMSH is 2D. Elevation coordinates need to be specified either using hardwired code or the tool introduced in this section. The input is the 2D mesh file and the DEM data. For each node in the mesh, this tool will loop over all DEM points to find the nearest one and assign the elevation to the node. For large data set, it's better to use parallel interpolations using OpenMP which is implemented in the code. User can se up the number of processors and run the interpolation in parallel.

Bibliography

K. Anastasiou and C.T. Chan. Solution of the 2d shallow water equations using the finite volume method on unstructured triangular meshes. *International Journal for Numerical Methods in Fluids*, 24:1225–1245, 1997.

Christophe Geuzaine and Jean-François Remacle. *Gmsh: a three-dimensional finite element mesh generator with built-in pre- and post-processing facilities*, 2009.

N Goutal and F Maurel. Proceeding of 2nd workshop on dam-break wave simulation. France, 1997.

A.J. Grass. Sediment transport by waves and currents. Technical Report FL29, SERC London Center for Marine Technology, 1981.

J. Hudson and P.K. Sweby. A high-resolution scheme for the equations governing 2d bed-load sediment transport. *International Journal for Numerical Methods in Fluids*, 47:1085–1091, 2005.

X. Liu. Numerical simulation of dike break process and sediment parametric determination in the lower yellow river. Master's thesis, Peking University, 2003.

X. Liu. *Numerical Models for Scour and Liquefaction around Object under Currents and Waves*. PhD thesis, University of Illinois at Urbana and Champaign, 2008.

X. Liu and M.H. Garcia. Discussion of "divergence form for bed slope source term in shallow water equations" by a. valiani and l. begnudelli. *Journal of Hydraulic Engineering*, 134(5): 678–679, 2008a.

X. Liu and M.H. Garcia. A 3d numerical model with free water surface and mesh deformation for local sediment scour. *Journal of Waterway, Port, Coastal, and Ocean Engineering*, 134(4): 203–217, 2008b.

X. Liu and M.H. Garcia. Coupled two-dimensional model for scour based on shallow water equations with unstructured mesh. *Coastal Engineering*, 55(10):800–810, 2008c.

X. Liu and G. Parker. Modeling of hydrodynamics and sediment transport in St. Clair River. submitted to International Joint Commission, International Upper Great Lakes Study, Department of Civil and Environmental Engineering, University of Illinois at Urbana-Champaign, 2009.

E. Meyer-Peter and R. Muller. Formulas for bedload transport. In *Proceedings of* 2^{nd} *Congress, International Association for Hydraulic Research*, pages 39–64, Stockholm, 1948.

P.L. Roe. Approximate riemann solvers, parameter vectors and difference schemes. *Journal of Computational Physics*, 43:357–372, 1981.

P.L. Roe. Characteristic based schemes for the euler equations. *Ann. Rev. Fluid. Mech*, 18: 337–365, 1986.

B. Rogers, M. Fujihara, and A.G.L. Borthwick. Adaptive q-tree godunov-type scheme for shallow water equations. *International Journal for Numerical Methods in Fluids*, 35:247–280, 2001.

B.D. Rogers, A.G.L. Borthwick, and P.H. Taylor. Mathematical balancing of flux gradient and source terms prior to using roe's approximate riemann solver. *Journal of Computational Physics*, 192:422–451, 2003.

T.H. Yoon and S. Kang. Finite volume model for two-dimensional shallow water flows on unstructured grids. *Journal of Hydraulic Engineering*, 130(7):678–688, 2004.